Integration of Flow Dependent Relative Permeability Maps for Two-Phase Flows in Porous Media into the COMSOL Multiphysics™ Earth Science Module

Marios S. Valavanides*[1], Eugene D. Skouras [2,3], Alexandros N. Kalarakis [2,3], Vasilis Burganos[2]
[1]TEI Athens, [2]FORTH/ICE-HT, [3]TEI Western Greece
* Applied Mechanics Laboratory, Dept. of Civil Engineering, TEI Athens, Ag. Spyridonos, GR-12210 Athens, Greece, marval@teiath.gr

Abstract[1]: True-to-mechanism relative permeability maps for steady-state two-phase flow in porous media were integrated within the COMSOL™ Earth Science module, to resolve field-scale flows. The essential characteristic of relative permeability dependence on local flow conditions (capillary number and flowrate ratio) have been provided by the *DeProF* model and associated theory.
The flow dependent relative permeability maps have been incorporated in the Earth Science module and an appropriate modeling strategy has been contrived to treat the actual two-phase flow problem as a an equivalent "effective-phase" (1-ph) flow problem.
Various flow arrangements, considering gravity effects and sources/sinks have been simulated. The simulations showed that the integration scheme is stable, it converges and numerical instabilities are only localized in areas where flow concentration takes extremely high values (as expected).
Keywords: Two-phase flow, porous media, relative permeability, simulators, field scale.

1. Introduction

Two-phase flow in porous media is a physical process whereby two phases simultaneously flow within a porous medium. When the flow is immiscible (i.e. the two phases do not mix), one of the phases ("water") is wetting the interstitial surface of the porous medium against the other, non-wetting phase ("oil"). The combined effect of wetting and interfacial tension is the disconnection of the non-wetting phase into fluidic elements of smaller or larger size – compared to the average pore size. Two-phase flow in porous media occupies a central position in physically important processes with practical applications of industrial and environmental interest, such as: enhanced oil recovery [1], carbon dioxide sequestration [2], groundwater and soil contamination and subsurface remediation [3], the operation of multiphase trickle-bed reactors [4], the operation of proton exchange membrane fuel cells [5], etc. The majority of those applications are based on inherently transient processes whereby one phase displaces the other, e.g. drainage -oil enters the pore network to displace water, or imbibition -if water displaces oil. In addition, averages of physical quantities -taken over any volume larger than the representative elementary volume (REV)- change with position and time. For example, the average saturation of the wetting phase over any region of the pore network increases with time as water is replacing oil during the imbibition process.

1.1 Two-phase flow relative permeabilities

The concept of relative permeability is basic when the two immiscible phases flow simultaneously within a porous medium. It has been contrived to extend Darcy's law in accounting the phenomenology of the process. The so-called fractional form of Darcy's law is

$$\tilde{U}_i = k_{ri}\frac{\tilde{k}}{\tilde{\mu}_i}\left(-\frac{\Delta\tilde{p}}{\Delta\tilde{z}}\right)_i \qquad i = o, w \qquad (1)$$

where $\tilde{U}_o$ and $\tilde{U}_w$ are the superficial velocities of oil (the non-wetting phase) and water (the wetting phase), e.g. oil/water, gas/oil, etc; $\tilde{\mu}_o, \tilde{\mu}_w$ are the dynamic viscosities of the two phases and $\left(-\Delta\tilde{p}/\Delta\tilde{z}\right)_i$ represents the macroscopic pressure gradient in each phase, i=o,w. The relative permeability of oil and water (dimensionless) are denoted by k_{ro} and k_{rw} respectively.

In general, relative permeabilities are measured either by *steady-state* or *unsteady-state* methods [6]. In steady-state methods, the two-

[1] Presented at the **COMSOL 2015 Conference**, Grenoble, Oct., 14-16

phases are simultaneously injected at a fixed ratio into a porous medium. When the system reaches steady-state conditions (averages do not change with time), the differential pressure and the saturation (by convention) of the wetting phase, S_w, are measured and the relative permeabilities can be calculated by using Darcy's law, eqn. (1). Steady-state methods are in general relatively accurate, easy to understand and implement straightforward and acceptable data processing procedures, namely regular/special core analysis (R/SCAL). However, since the process needs to reach steady-state conditions it is, in general, time-consuming. Relative permeability curves are produced for a given porous medium and for a given pair of fluids by laboratory measurements when different flow conditions are imposed.

Diagrams of relative permeabilities provide valuable and necessary data input in reservoir studies when estimating the producible reserves and design flooding/sweeping interventions for ultimate recovery.

2. The DeProF mechanistic model

The mechanistic model *DeProF* [7], predicts the relative permeability of oil and water in terms of the capillary number, *Ca*, the oil/water flowrate ratio, *r*, the oil/water viscosity ratio, *M*, the advancing and receding contact angles, and a parameter vector, comprising the dimensionless geometrical and topological parameters affecting the flow.

The *DeProF* model is the first mechanistic model describing the flow in terms of its actual independent variables, Ca, and r. It shows improved performance over the conventional modeling of saturation-described flow. Not only the *DeProF* model matches the process phenomenology with a remarkable specificity, but it also reveals latent phenomenology, e.g. the existence of optimum operating conditions. The latter has been recently confirmed by a major re-examination of laboratory studies [8] and is justified on the basis of statistical thermodynamics principles [9]. In that context, the *DeProF* theory provides a deeper and more accurate (true-to-mechanism) description of the sought process and the underlying mechanisms.

Using the *DeProF* model, one can obtain the solution to the problem of steady-state two-phase flow in porous media in the form of the following transfer function

$$x = x\left(Ca, r; \kappa, \theta_A^0, \theta_R^0, \mathbf{x}_{pm}\right) \qquad (2)$$

where, $x = \left(-\partial\tilde{p}/\partial\tilde{z}\right)\tilde{k}\left(\tilde{\gamma}_{ow}Ca\right)^{-1}$ is the reduced macroscopic pressure gradient, $\tilde{k}$ is the absolute permeability of the porous medium, Ca is the capillary number, defined as $Ca = \tilde{\mu}_w\tilde{U}_w/\tilde{\gamma}_{ow}$ ($\tilde{\mu}_w$ is the viscosity of water, $\tilde{U}_w$ is the superficial velocity of water, and $\tilde{\gamma}_{ow}$ is the interfacial tension), $r = \tilde{q}_o/\tilde{q}_w$ is the oil/water flowrate ratio, $\kappa = \tilde{\mu}_o/\tilde{\mu}_w$ is the oil/water viscosity ratio, θ_A^0 and θ_R^0 are the advancing and receding contact angles and $\mathbf{x}_{pm}$ is a parameter vector composed of all the dimensionless geometrical and topological parameters of the porous medium affecting the flow (e.g. porosity, genus, coordination number, normalized chamber and throat size distributions, chamber-to-throat size correlation factors, etc). In the definition of the reduced macroscopic pressure gradient, the term $\left(\tilde{\gamma}_{ow}Ca\right)/\tilde{k}$ represents the pressure gradient for one-phase flow of water at superficial velocity $\tilde{U}_w$. Note that in equation (2) S_w is not considered to be an independent variable; actually, S_w is one of the dependent variables in the system of *DeProF* equations. A typical dependence of x on Ca & r is presented in Figure 1.

Extended simulations with the *DeProF* model algorithm in a 3D pore network of the chamber-and-throat type, delivered macroscopic, reduced pressure gradient maps, *x*, expressed in the form of a scaling law function of Ca & r, x(Ca,r), Figure 1 pertaining to a system with o/w viscosity ratio $\kappa = 1{,}45$. Actually, the *DeProF* simulator predicts values for the reduced pressure gradient, $x_{ij}(Ca_i,r_j)$ over a grid of Ca_i and r_j values. The idea is to fit those values by a functional form x(Ca,r),

The reduced pressure gradient, eqn (2) may be fitted by a general expression of the form

$$x\left(Ca, r\right) = \begin{cases} A(r)\left(10^6 Ca\right)^{-B(r)} & r \le r_{lim}\left(Ca\right) \\ n/a & r > r_{lim}\left(Ca\right) \end{cases} \qquad (3)$$

where

$$A(r) = 10^{\sum_{i=0}^{3} A_i (\log r)^i} \quad (4)$$
$$= 10^{A_0 + A_1 \log r + A_2 (\log r)^2 + A_3 (\log r)^3}$$

and

$$B(r) = \sum_{i=0}^{3} B_i (\log r)^i \quad (5)$$
$$= B_0 + B_1 \log r + B_2 (\log r)^2 + B_3 (\log r)^3$$

are functions of r and A_i, B_i, i=0,..,3 are appropriate coefficients, that take values according to the system parameters, and

$$r_{lim}(Ca) = 10^{C(\kappa) Ca^{D(\kappa)}} \quad (6)$$

are the limiting values of the flowrate ratio, r, for which two-phase flow is sustainable.

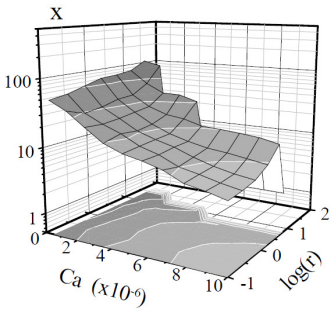

Figure 1. Typical reduced pressure gradient map, x(Ca,r), over the domain of flow conditions, the capillary number, Ca and the flowrate ratio, r.

The values of the coefficients in eqs (3)-(6), for typical steady-state two-phase flows of an oil-water system within a pore network are presented in Table 1. The values pertain to typical simulations of steady-state oil/water flow (with viscosity ratio, $\kappa = 1{,}45$), within the ball-and-stick 3D network described in [10]. The x(Ca,r) map described by eqs(3)-(6) and the coefficient values in Table 1, was integrated into the COMSOL™ Earth Science module.

Table 1 Values of the coefficients in the reduced pressure gradient x(Ca,r) [eqs (11)-(14)]

Viscosity ratio, $\kappa = 1{,}45$				
i	**A_i**	**B_i**	**C**	**D**
0	1,5218	0,7215	1,7786	-0,3726
1	0,0766	-0,1356	--	--
2	0,1090	-0,0037	--	--
3	0,0332	0,0035	--	--

3. Use of COMSOL Multiphysics

A lean integration scheme capable of handling steady-state two-phase flow problems was developed. The COMSOL™ Earth Science module [11] is dodged by treating the two-phase flow problem as an equivalent one-phase flow problem of a virtual fluid having a local effective mobility equal to the sum of the local mobilities of oil and water. Inflows/outflows to/from the control volume of either fluid, whether oil or water, are treated as equivalent flowrates of effective fluid (equivalent one-phase). The tricky point here is that the computational scheme (conceptual algorithm) cannot support complete saturation and in this context, injection of one phase needs to be "spoiled" with some insignificant flowrate of the other phase.

The algorithm solves the equivalent 1-ph flow problem combining Darcy's law with the continuity equation and the transport equation for the apparent fluid density and viscosity, calculated as saturation-weighted averages of oil/water properties, while considering dependence of the effective hydraulic conductivity on local flow conditions. The latter are described by the total flowrate intensity (effective superficial velocity), equal to the sum of oil and water velocities.

For a local set of oil and water velocities, the local values of *Ca* & *r* are readily computed and the local effective mobility is estimated as the sum of the local oil & water mobilities. These, and the reduced pressure gradient, are looked-up from the *DeProF* map for the corresponding *Ca*, *r* values. Implementation of the standard Darcy velocity *vs* pressure gradient relation for the equivalent phase, delivers the new effective superficial velocity. This latter is decomposed into a set of local oil & water superficial velocities according to the value of the flowrate ratio. The procedure is repeated along the effective flow streamlines which coincide with the actual 2-ph flow streamlines.

We need to stress here that, to the authors knowledge it is the first time flow dependent relative permeability maps are incorporated in a two-phase flow simulator.

4. Results

The integration scheme just described in Section 3, has been applied to a variety of injection/production patterns. Here we present

two indicative cases: A waterflood in a 7-spot arrangement, and annular sleeve driven waterflood.

4.1 Water flood in a 7-spot arrangement

The basic geometry of a 7-spot arrangement is depicted in Figure 2. Ideally, a 7-spot arrangement is made up of many adjacent hexagonal right cylindrical prisms of the same size, forming a honeycomb structure [12, 13]. Each hexagonal prism comprise a rectilinear producer (sink) surrounded by 6 parallel rectilinear injectors (sources), running perpendicular to the figure plane. Water is pressed through the injection wells (sources, ⊕) to drive and sweep the oil-in-place to the producers production wells (sinks,⊗). Gravity effects are neglected. The formation is considered homogeneous (porosity, absolute permeability, pore network structure etc). Because of the particular geometry, the porous medium homogeneity and uniformly injected water, 12 identical flow patterns are formed (as a kaleidoscope image). Each flow pattern is confined within a 90-30-60 right triangle.

Figure 3 presents indicative snapshots of the simulated 7-spot water flooding within the arrangement just described. Water is continuously injected from the source located at the 60 deg corner and drives the oil in place into the sink located on the 30 deg corner. The simulation is carried over a hexagonal formation of size (refer to Fig. 1, radius l=2000m). The left column diagrams in Fig. 3 provide snapshots of saturation maps at 500 days (top) and 1000 days (bottom) after injection start, for 0,1bar pressure difference. The diagrams on the right column provide the corresponding saturation maps for water drive at 10 times higher pressure difference (1,0 bar). The simulation indicates water breakthrough is to happen at ~1000 days. Videos showing the whole flooding process (start to complete sweeping) for the two different values of pressure drive (i.e. for 8000days and 3000 days) can be downloaded through the following hyperlinks:

ΔP=0,1bar →
http://users.teiath.gr/marval/ArchIII/DeProF_2Dslice_Pin=0.1atm_8000d.avi

ΔP=1,0bar →
http://users.teiath.gr/marval/ArchIII/DeProF_2Dslice_Pin=1.0atm_3000d.avi

One may notice numerical instabilities at the vicinity of the sink (bottom corner) after water breakthrough has occurred. This is attributed to the mesh size. In essence, the instabilities (colour variations) reveal the size of the mesh. Resizing the mesh or, equivalently, increasing the well diameter, reduces the problem. We stress here that those slight numerical instabilities occur exclusively around sinks (or sources).

4.2 Deep annular sleeve waterflood

Figure 4 presents the case study, whereby water is continuously injected from an annular sleeve on the bottom of a cylindrical formation and drives the initial oil-in-place towards the extraction well, located in the centre of the cylinder. The cylindrical formation has a radius of r=1,0km and extends underground between two horizontal planes from a depth $z=z_0=5$ (ABCD) to a depth $z=z_0+3km=8km$ (IJKL). It is surrounded by a 10m thick annular sleeve (BCDLKJ). Water imbibes into the formation through the entire cylindrical surface FGHLKJ) at the bottom of the sleeve, extending from a depth of 7km (EFGH) to 8 km (IJKL), whereas the rest of the cylindrical surface (BCDHGF), spanning over 5 to 7 km depths, is considered to be impervious. The annular sleeve is kept at fixed water saturation $S_w=0,9$ and at hydrostatic pressure $P_{in}(z)=\rho g(z_0+z)+\Delta P$ (inlet conditions). Gravity effects are taken into account. The circular cross-section at the bottom of the cylindrical formation (IJKL) is kept at fixed oil saturation conditions, $S_o=0,9$ (the whole surface is considered to be a source of oil replenishing the original oil-in-place swept by the waterflood. The (hydrostatic) pressure distribution along the extraction well is given by $P_{out}(z)=\rho g(z_0+z)$ (Outlet conditions). The diagrams in Figure 4 depict the flow conditions (4a), a 3D impression of the cylindrical formation (4b, showing the annular sleeve, the injection surface and production well), and a snapshot (4c) taken from the simulation (showing the saturation map obtained over the wedge sliced out of the cylindrical control volume). A video showing the particular flooding arrangement is available: http://users.teiath.gr/marval/ArchIII/DeProF_Depth_Pin=10atm_35d.avi

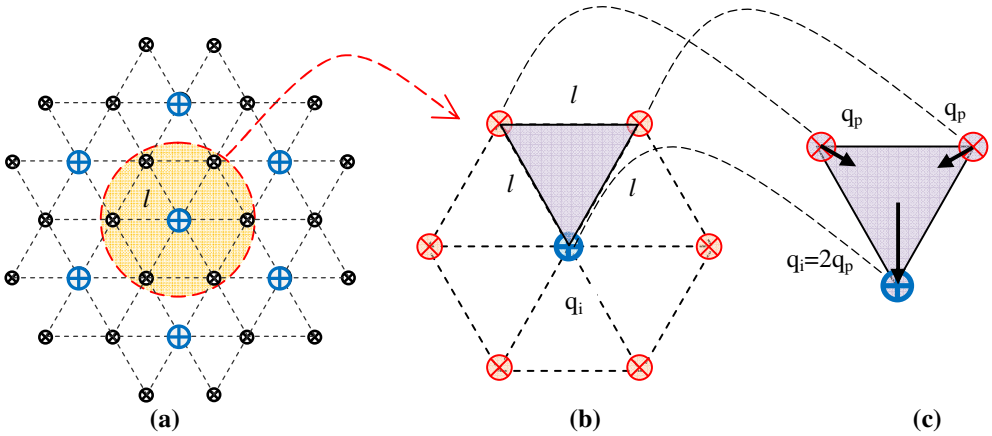

Figure 2 Modular break-down of a 7-spot pattern well pattern formation **(a)** Layout of the 7-spot formation of water injection wells ("sources", ⊗) and oil/water production wells ("sinks", ⊕). The honeycomb pattern extends infinitely in both directions. **(b)** The 7-spot pattern hexagonal building block **(c)** the modular unit cell (equilateral triangle)

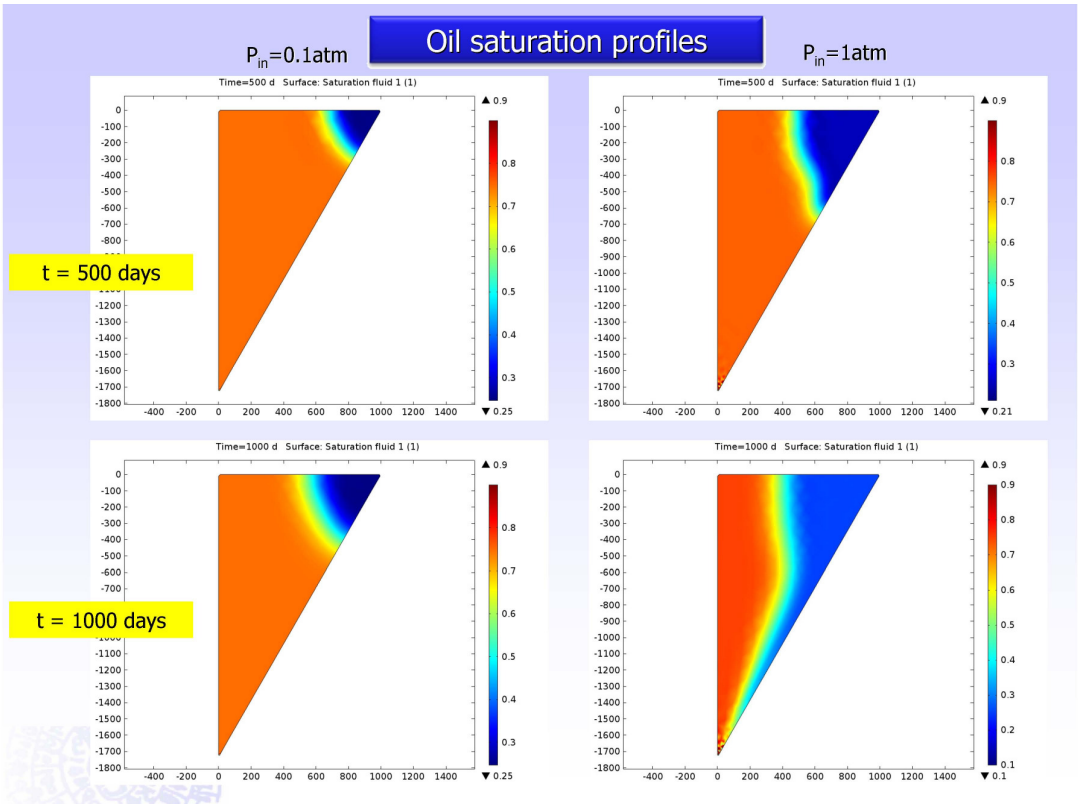

Figure 3. Typical simulation snapshots pertaining to 7-spot water flooding of an oil-saturated formation (see Fig.2). Triangles are the building blocks (control volume elements) of the 7-spot layout. Sides are impermeable. Water is injected at the top, acute corner (source). Oil (initially) and oil/water (after breakthrough) are extracted from the bottom corner (sink). (a) Low drive pressure difference (b) Increased (×10) pressure difference. Videos are available for:
ΔP=0,1bar → http://users.teiath.gr/marval/ArchIII/DeProF_2Dslice_Pin=0.1atm_8000d.avi
ΔP=1,0bar → http://users.teiath.gr/marval/ArchIII/DeProF_2Dslice_Pin=1.0atm_3000d.avi

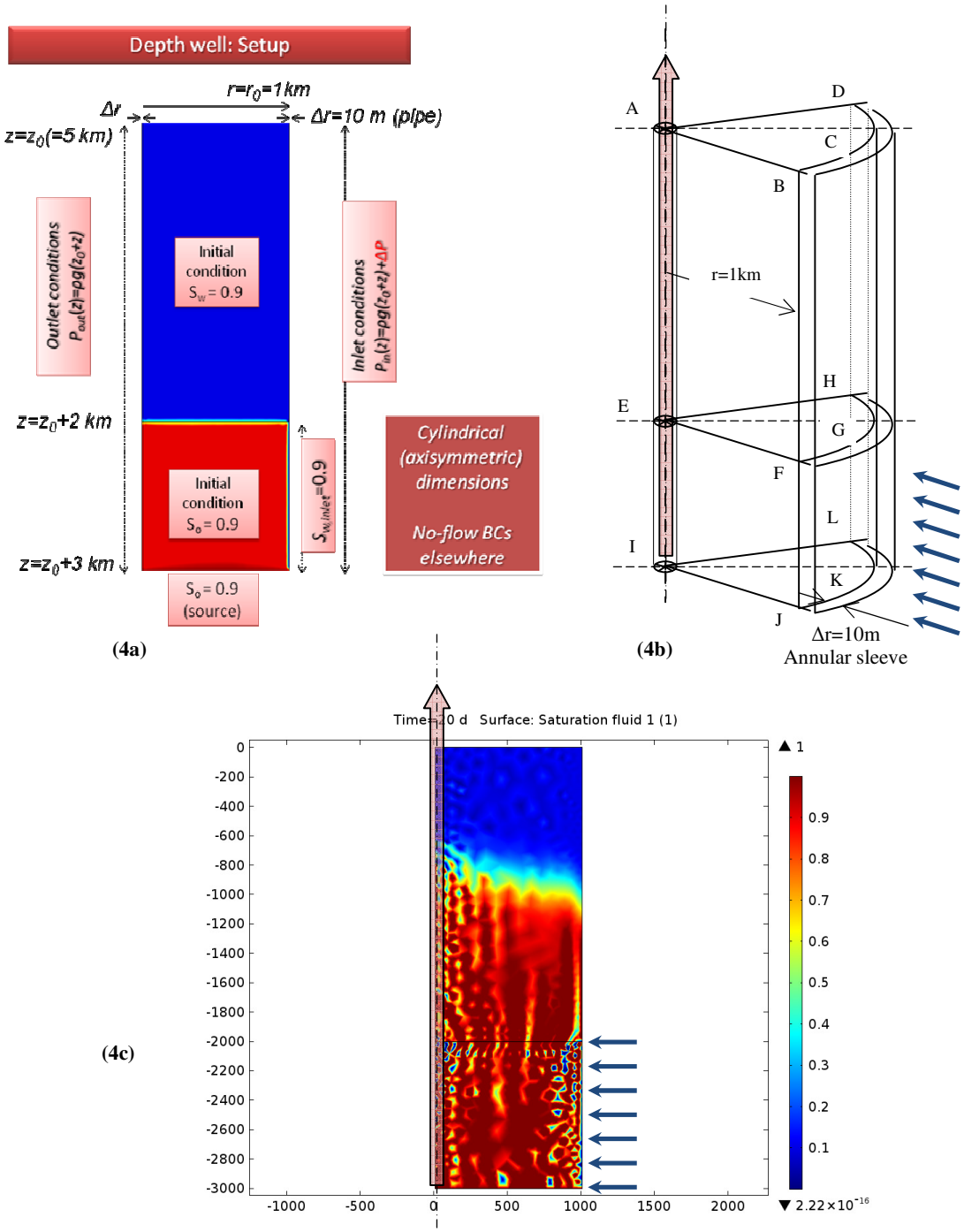

Figure 4. Bottom annular sleeve water drive arrangement (a)flow conditions, (b) 3D impression of the cylindrical formation showing the annular sleeve, the injection surface and production well, (c) snapshot taken from the simulation showing the saturation map obtained over the wedge sliced out of the cylindrical control volume. Videos is available http://users.teiath.gr/marval/ArchIII/DeProF_Depth_Pin=10atm_35d.avi

8. Conclusions

Functional forms of two-phase flow in porous media relative permeability derived from the *DeProF* true-to-mechanism model have been used to simulate various waterflooding arrangements. The essential characteristic of relative permeability dependence on the local flow conditions have been provided by the *DeProF* model and associated theory. Local flow conditions pertain to superficial velocities of oil and water or, equivalently, capillary number and flowrate ratio.

The flow dependent relative permeability maps have been incorporated in the COMSOL™ Earth Science module and an appropriate modeling strategy has been contrived and implemented to treat the actual two-phase flow problem as a an equivalent "effective-phase" (1-ph) flow problem. The simulations showed that the integration scheme is stable, it converges and numerical instabilities are only localized in areas where flow concentration takes extremely high values (as expected).

It is now possible to develop more efficient and more reliable simulators incorporating the actual physics of two-phase flow in porous media processes.

9. References

1. Lake, L. W., "*Enhanced Oil Recovery*", Prentice-Hall, Englewood Cliffs, NJ (1989)
2. Burnside, N.M. Naylor, M., "Review and implications of relative permeability of CO2/brine systems and residual trapping of CO_2", *International Journal of Greenhouse Gas Control* **23,** 1–11 (2014)
3. Khan, F.I., Husain, T., Hejazi, R., "An overview and analysis of site remediation technologies", *Journal of Environmental Management* **71**, 95–122 (2004)
4. Van de Merwe, W., Nicol, W., "Trickle flow hydrodynamic multiplicity: Experimental observations and pore-scale capillary mechanism", *Chemical Engineering Science* **64**, 1267–1284 (2009)
5. Bazylak A., "Liquid water visualization in PEM fuel cells: A review", *International Journal of Hydrogen Energy,* **34**(9), 3845-3857 (2009)
6. Honarpour, M., Koederitz, L., Harvey, A.H., "Relative Permeability of Petroleum Reservoirs", Boca Raton, Florida, USA, CRC Press, ISBN 0-8493-5739-X (1986)
7. Valavanides, M.S. "Steady-State Two-Phase Flow in Porous Media: Review of Progress in the Development of the DeProF Theory Bridging Pore- to Statistical Thermodynamics- Scales" *Oil & Gas Science and Technology* **67**(5), 787-804 (2012) [http://dx.doi.org/10.2516/ogst/2012056]
8. Valavanides, M., Totaj, E., Tsokopoulos, M., "Energy efficiency Characteristics in Steady-State Relative Permeability Diagrams of Two-Phase Flows in Porous Media" *Journal of Petroleum Science and Engineering* PETROL-S-15-00701, in press (2015)
9. Daras, T., Valavanides, M., "Number of Microstates and Configurational Entropy for Steady-State Two-Phase Flows in Pore Networks" *AIP Conf. Proc.* **1641**, 147-154 (2015) http://dx.doi.org/10.1063/1.4905973
10. Valavanides, M.S., Payatakes, A.C. "Effects of Pore Network Characteristics on Steady-State Two-Phase Flow Based on a True-to-Mechanism Model (*DeProF*)" SPE78516, *10th ADIPEC Abu Dhabi International Petroleum Exhibition & Conference, Abu Dhabi*, UAE, 379-387 (2002)
11. COMSOL Multiphysics *Earth Science Module User's Guide* , © 1998–2008 by COMSOL AB. All rights reserved, Version: November 2008, COMSOL 3.5a
12. Langnes, G.L., Robertson, J.O., Mehdizadeh, A., Torabzadeh, J. "Waterflooding" in "Enhanced Oil Recovery I, Fundamentals and Analyses (Developments in Petroleum Science; 17A)" Donaldson, E.C. , Chilingarian, G.V., Yen, T.F. (Editors), ISBN 0444-42206-4 Elsevier Science Publishers B.V. pp. 260-262 (1985)
13. Valavanides, M.S., Skouras, E.D., "Rational solitary well spacing in soil remediation processes" *Fresenius Environmental Bulletin* **23**(11), 2847-2851 (2014)

10. Acknowledgements

This research has been co-financed by the European Union (European Social Fund – ESF) and Greek national funds, Operational Program "Education and Lifelong Learning" of the National Strategic Reference Framework (NSRF) - Research Funding Program: **ARCHIMEDES III**. Investing in knowledge society through the European Structural Fund.

Review and comments from T. Kokkinos, TEI Athens, are greatly acknowledged.